Jadwiga Zalewska, Marek Dohnalik
Oil and Gas Institute, Krakow

Comparison of rock pore space based on X-ray computed microtomography (micro-CT) and nuclear magnetic resonance (NMR) data. Part III

Introduction

The exploratory works for creating gas reservoirs in Poznań region have been carried out for many years. The sandstones originating from Rotliegend formations are the reservoir rock in this region. They are characterized by low and very low reservoir properties, which constitutes a significant problem in the zone under examination. The causes of this phenomenon are currently under research. Leśniak at al. [2] accomplished a study ordered by PGNiG, in which diagenesis influence on reservoir parameters and petrographic characteristics of this sandstones was discussed. The results obtained in above-mentioned study were used for mineralogical – petrographical and reservoir interpretation of samples presented in this study whose aim was evaluation of Rotliegend Aeolian sandstones pore space based on X-ray computed microtomography (micro-CT) and nuclear magnetic resonance (NMR) data. Combining the data from both methods enabled us to obtain valuable information on porosity, pore size distribution, as well as the distribution of their saturation, and made possible evaluation of the actual reservoir properties of the rocks.

Results

The analysis of NMR results for samples from discussed region was presented in Zalewska et al. [4]. Then, graphs of cumulative NMR signals, normalized in relation to the maximum value were prepared, which were set up in T_2 relaxation times relationship, because they characterize the behavior of hydrogen nuclei in the rock pore space (according to the work of Jarzyna et al. [1]). Distributions of transverse relaxation times in individual rock samples were prepared, divided subsequently into concave, convex and constant slope curves. Concave curves of T_2 distribution correspond to the rocks in which smaller pores or fractures predominate; convex curves are typical of the rocks in which media migration proceeds in pores or fractures of large diameters, while constant slope curves give evidence that pore space has diversified diameters [1].

Figure 1 and 4 present cumulative and normalized NMR signals obtained for all examined samples. Colors were differentiated in order to qualitatively compare signals for samples originating from individual wells: the red color curves are for samples originating from G-1 well, navy blue curves represent O-3 well, while yellow curves represent the R region. When analyzing the first group of graphs, visualizing concave curves (Figure 1) one can find that R region (yellow color) features small diameter pore system in majority of cases, which is represented in this collection by 7 samples. The following samples are distinguishable by the poorest reservoir parameters: No. 10734 (G-1 well) and No. 10746 (O-3 well), for which T_2 transverse relaxation time distribution is illustrated in Figure 2. Figure 3 presents the percentage of individual pore classes in pore space volume of the sample. The three samples were representatives of P2 facies sandy playa, represented by fine- and very fine-grained sandstones.

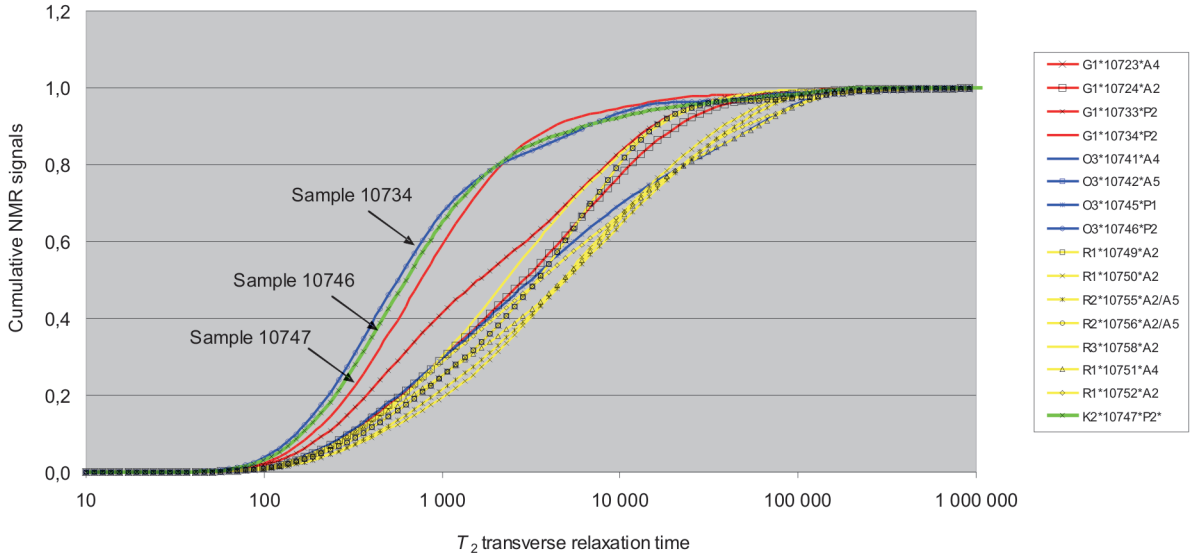

Fig. 1. Comparison of cumulative NMR signals for analyzed samples – concave curves

samples from well G-1 – in red, well O-3 – navy blue, R-region – yellow, sample from K-2 well – green

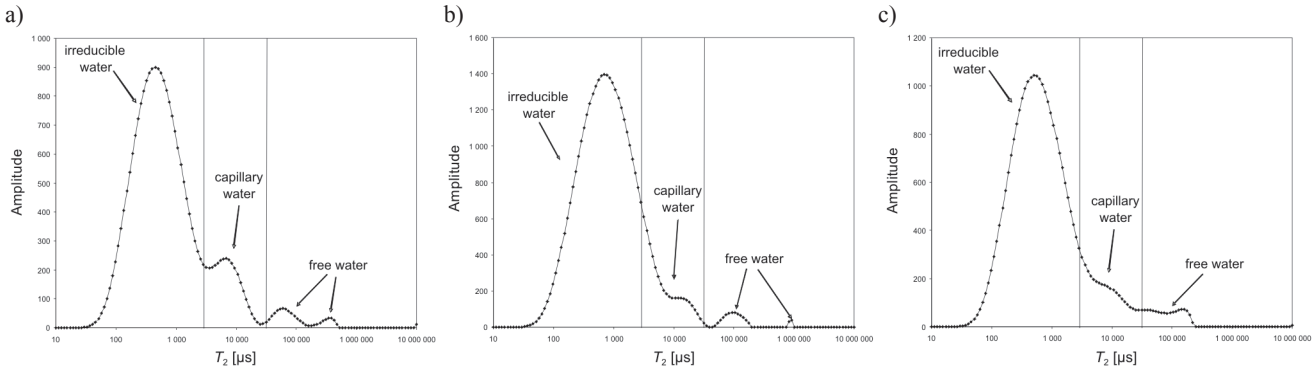

Fig. 2. Model distributions of T_2 transverse relaxation time representing the poorest reservoir parameters

a) 10734 sample from G-1 well, P2 facies; b) 10746 sample from O-3 well, P2 facies; c) 10747 sample from K-2 well, P2 facies

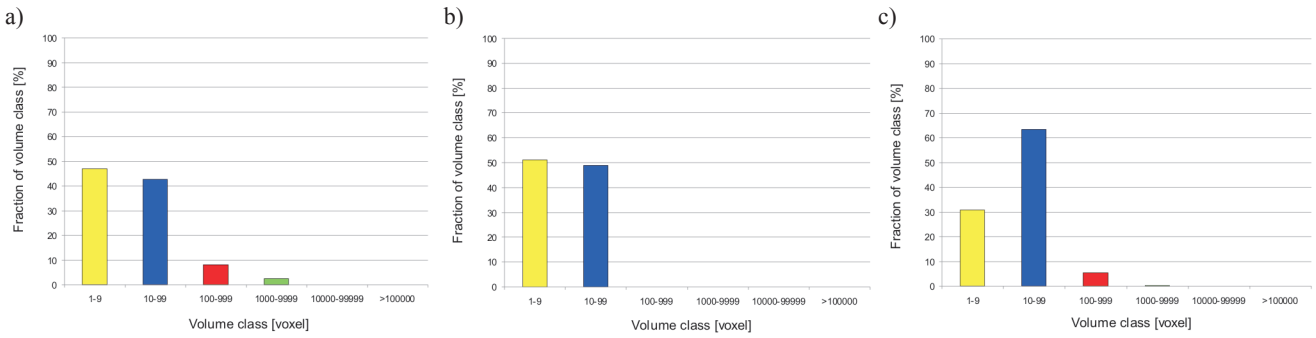

Fig. 3. Graphs of volume class percentages based on tomographic data for samples of the poorest reservoir properties

a) 10734 sample from G-1 well, P2 facies; b) 10746 sample from O-3 well, P2 facies; c) 10747 sample from K-2 well, P2 facies

While examining the second group of graphs illustrating the convex curves (Figure 4) characteristic for rocks in which large diameter pores predominate, one can state that all the samples are Aeolian dune sandstones of A2 facies. Samples from O-3 well (7) are distinguishable in the data set (Figure 4, navy blue color). Convex curves are also characteristic for samples from G-1 well (7 samples, Figure 4, red color), but they generally have slightly lower pore diameters than in O-1 well, except for samples 10729 and 10726. Figure 5 presents model distribution of T_2

transverse relaxation time for samples featuring the best reservoir properties: These are samples 10729 and 10726 (G-1 well), and sample 10743 (O-3 well). Figure 6 presents the percentage of individual pore volume classes within pore structure for the same samples as in Figure 5.

While analyzing NMR results for examined material from individual wells, shape diversification of T_2 curves can be observed. Two samples from G-1 well, representing the ceiling of examined formations (10734, 10733) and originating from P2 sandy playa facies, and two samples repre-

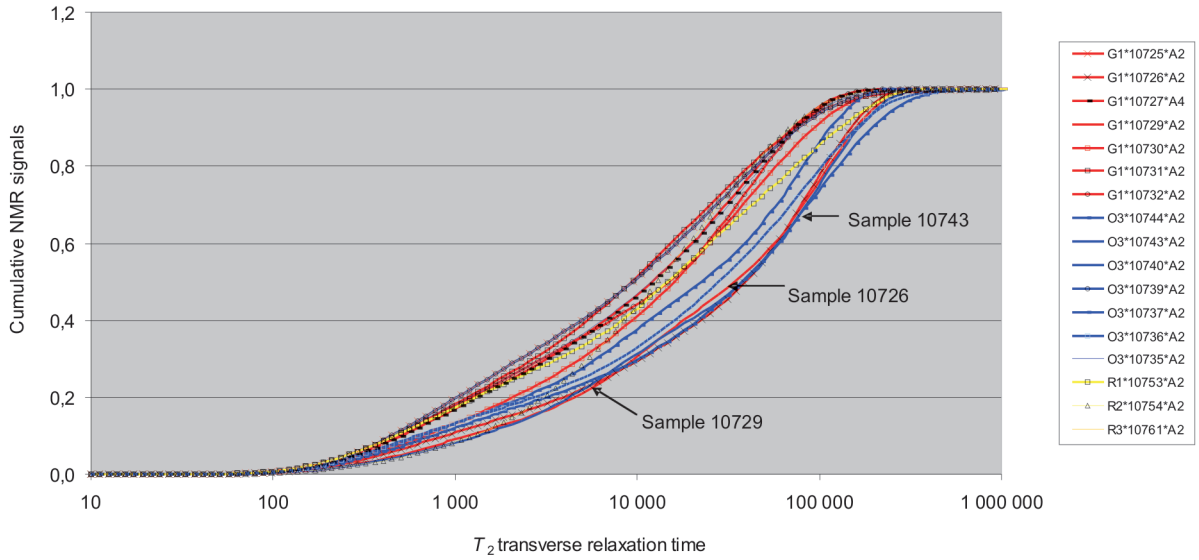

Fig. 4. Comparison of cumulative NMR signals for analyzed samples – convex curves
samples from G-1 well – in red, from O-3 well – navy blue, from R region – yellow

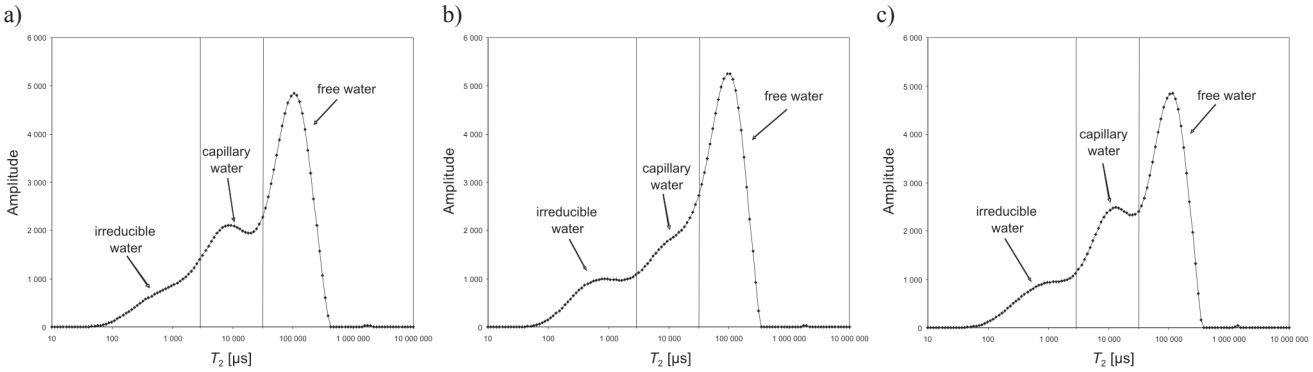

Fig. 5. Model distributions of T_2 transverse relaxation time representing the best reservoir parameters
a) 10729 sample from G-1 well, A2 facies; b) 10726 sample from G-1 well, A2 facies; c) 10743 sample from O-3 well, A2 facies

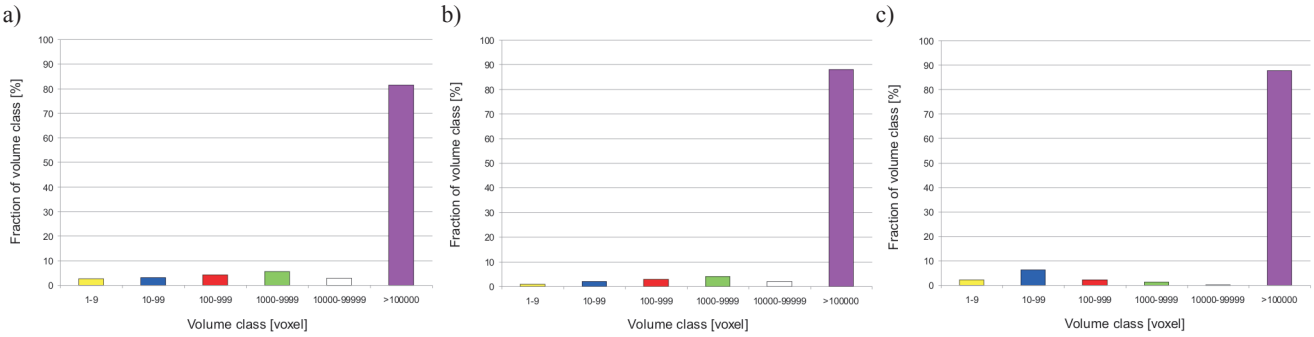

Fig. 6. Graphs of volume class percentages based on tomographic data for samples of the best reservoir properties
a) 10729 sample from G-1 well, A2 facies; b) 10726 sample from G-1 well, A2 facies; c) 10743 sample from O-3 well, A2 facies

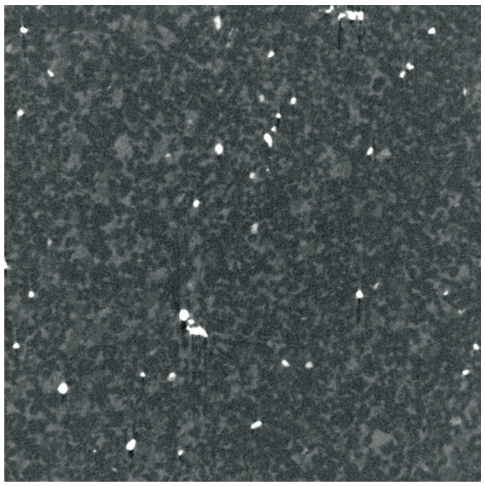

Fig. 7. Cemented pore space (light-grey phases) in sample 10733

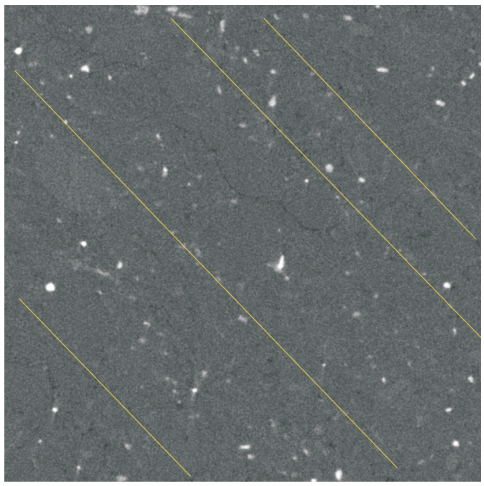

Fig. 8. Cross-section through sample 10723 with visible stratification (yellow color) and fissure (in the centre of the sample)

senting the bottom part – the first from A2 facies (10724) and the other from A4 facies (10723), show concave curve shape characteristic for rocks in which small size pores predominate. The remaining samples originating from this well (10725–10732) produce convex curves, giving evidence of large diameter pore occurrence. The samples listed above are Aeolian dune sandstones of A2 facies, with the exception of sample 10728 which was representative of A4 facies.

Microtomographic images also show that samples from this well, located within the ceiling of analyzed formation (samples 10734 and 10733), are characterized by low porosity, comprise of small pores ($2 \cdot 10^2 \div 2 \cdot 10^6$ µm^3 volumes), not connected to each other. Furthermore, it has been noted on micro-CT visualizations that strong cementation is present in samples belonging to P2 facies, which results in porosity decrease and was presented in Figure 7 (light-grey color). Moreover, distinctive alternating stratification of very fine grains, zone of cements and fissures in the centre was observed in two samples (10724, 10723) (Figure 8).

Figure 9 presents comparison of X-ray microtomography and nuclear magnetic resonance data for selected samples from G-1 well, representing rocks of good reservoir properties. The presence of pore assemblies belonging to VI volume class (volume higher than $2 \cdot 10^7$ µm^3), occupying a significant part of the pore space of the samples was noted in two samples of A2 facies (10730 and 10732). The subsequent two samples of A4 facies (10728–10727) represent, as regards tomography, the samples in which pore assemblies belonging to VI class are present, constituting, however, only a small fraction of pore space volume. Only in sample 10725 the correlation between tomography results and NMR examinations was not observed, which

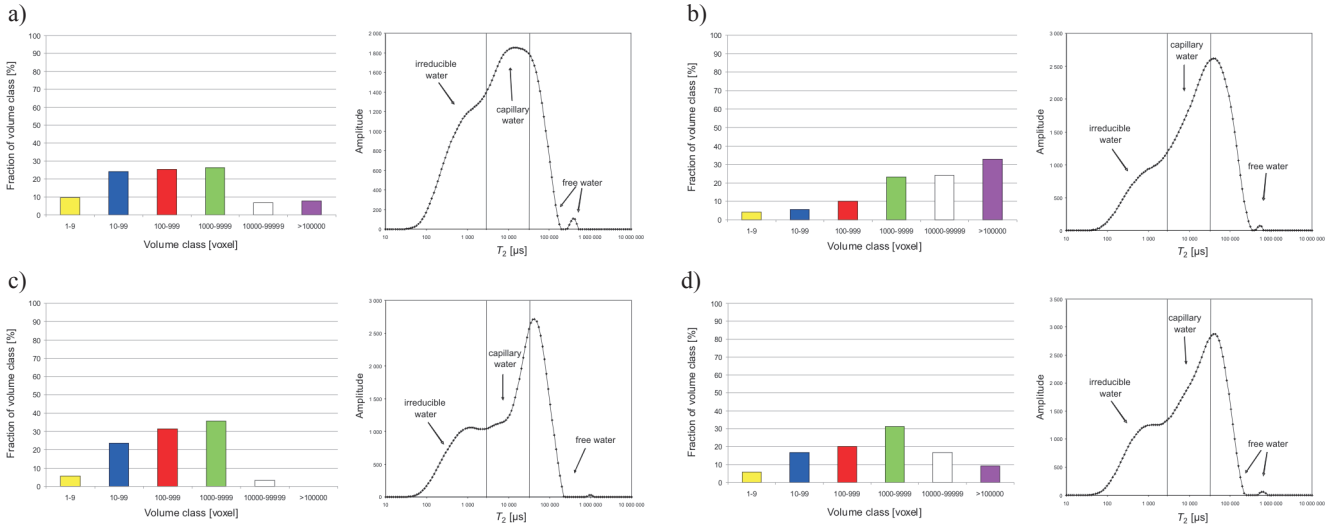

Fig. 9. Comparison of micro-CT and nuclear magnetic resonance data for selected samples from G-1 well

a) 10728 sample, A4 facies; b) 10730 sample, A2 facies; c) 10732 sample, A2 facies; d) 10727 sample, A4 facies

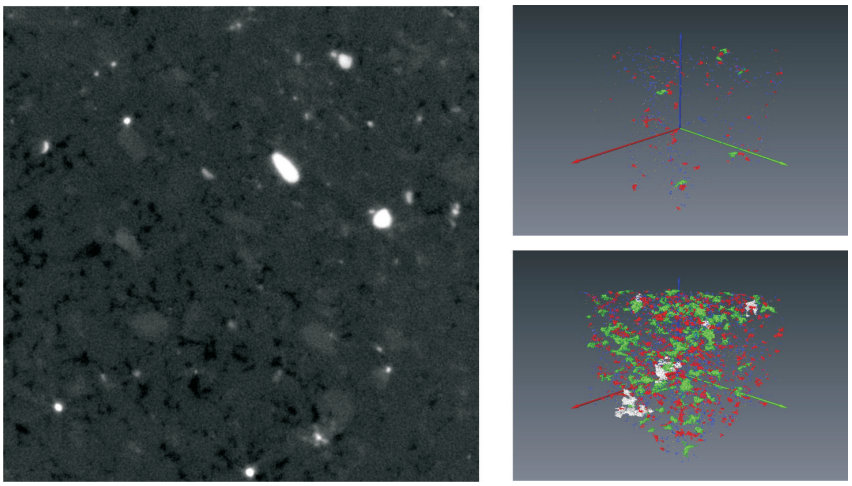

Fig. 10. Heterogeneity of pore space distribution in sample 10725

may result from high heterogeneity of pore distribution in this sample (Figure 10).

In O-3 well, as in the examples that have already been discussed, differentiation of NMR signal shapes for samples originating from this well section can be observed. Two samples representing the ceiling of examined formations (10746, 10745) are representatives of P2 facies sandy playa and P1 marginal playa respectively, two samples of Aeolian sandstones 10742 (A5 facies) and 10741 (A4 facies) show cumulative NMR signals as concave curves characteristic for rocks of small pore sizes.

The above results have been proved by results of X-ray microtomography examinations, which is illustrated in Figure 11. Samples 10746 and 10745, as well as 10742 and 10741 samples, have high fraction of pore classes of small volume ($2 \cdot 10^2 \div 2 \cdot 10^6$ µm^3), and are characteristic in total absence of objects belonging to the highest volume class VI.

The remaining samples from this well, representing Aeolian sandstones of A4 facies, produce cumulative NMR signals in the form of convex curves, testifying the occurrence of large diameter pores. Also, according to the results of microtomographic examinations, A2 facies sandstones have good reservoir properties. This can be evidenced by the presence of objects counted among class VI (pore volume higher than $2 \cdot 10^7$ µm^3) within the pore structure, constituting 10÷80% pore structure volume of the sample (Figure 12). The only exception here is sample 10738 which contains no objects from class VI of pore volume and features high percentage of classes I–III (volume $2 \cdot 10^2 \div 2 \cdot 10^5$ µm^3).

Sample 10743 features the best parameters, both according to NMR and micro-CT data, within this group of samples in which one pore of class VI constitutes 87%. In samples 10739 and 10740 the volume fraction of class VI is present at 20% level, while large pores from classes IV–V occupy approx. 40% of pore space (Figure 12a and 12b).

The only sample from O-3 well that does not correlate well between the two discussed measuring methods is sample 10744. It has high coefficient of effective porosity (Kp_{NMR_ef} = 10.8%) and according to micro-CT results it does not have good reservoir properties. As can be seen from graphical results (Figure 13), the pore structure of the sample comprises many small pores whose connections are probably below the resolution capacity of the microtomograph used (5.8 µm).

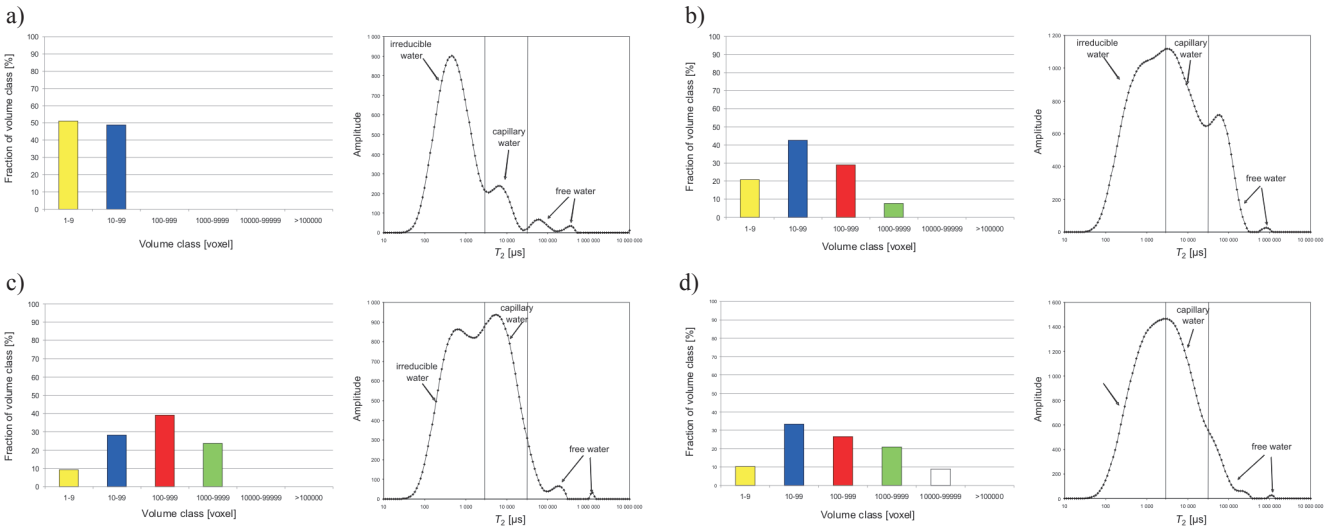

Fig. 11. Comparison of micro-CT and nuclear magnetic resonance data for selected samples from O-3 well

a) 10746 sample, P2 facies; b) 10745 sample, P1 facies; c) 10742 sample, A5 facies; d) 10741 sample, A4 facies

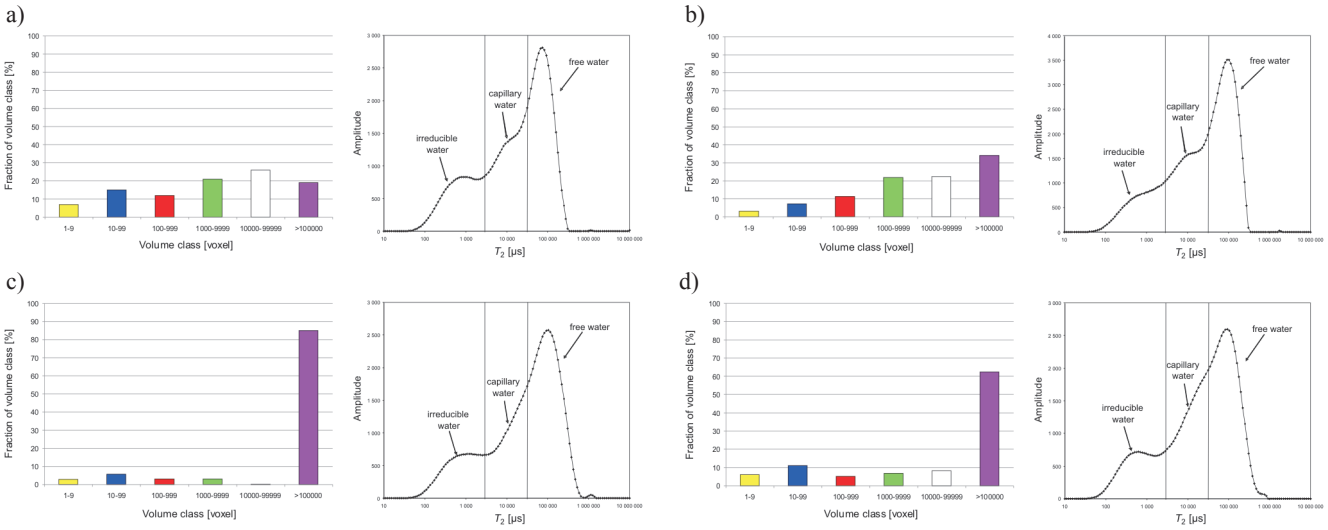

Fig. 12. Comparison of micro-CT and nuclear magnetic resonance data for selected samples from O-3 well, representing Aeolian sandstones of A2 facies

a) 10740 sample; b) 10739 sample; c) 10737 sample; d) 10736 sample

Only one, sample 10753 from R-1 well shows convex curve, giving evidence of the presence of slightly bigger diameter pores. The four remaining samples 10749, 10750, 10751, and 10752 produce concave curves, which is characteristic for weak reservoir rock properties.

Micro-CT examinations enabled us to determine that pores belonging to volume class VI (volume in excess of $2 \cdot 10^7$ µm^3) are not present in these samples (Figure 14b, c, d). Sample 10753 located at the bottom of the analyzed group of samples has much better properties. The largest pore assemblies belonging to volume class VI occupy 40% of the pore space in it (Figure 14a). The tomographic examination results correspond to the results obtained with NMR method.

The presence of very narrow, intermittent fissure (Figure 15) precluding its visualization was found in sample 10751.

Differentiation of transverse relaxation time distribution curves reflects heterogeneous nature of samples originating from R-2 well (Figure 16). Sample 10754 stands out in this set producing convex curve which indicates the occurrence of pores having larger diameters than those in the remaining samples. Sample10757 presents a curve of constant slope, which proves that pore space of this sample has diversified pore diameters. Two remaining samples, 10755 and 10756, produce concave curves, which gives evidence of small pores predominance in pore space construction (Figure 16). Both samples were marked with A2/A5 facies symbol.

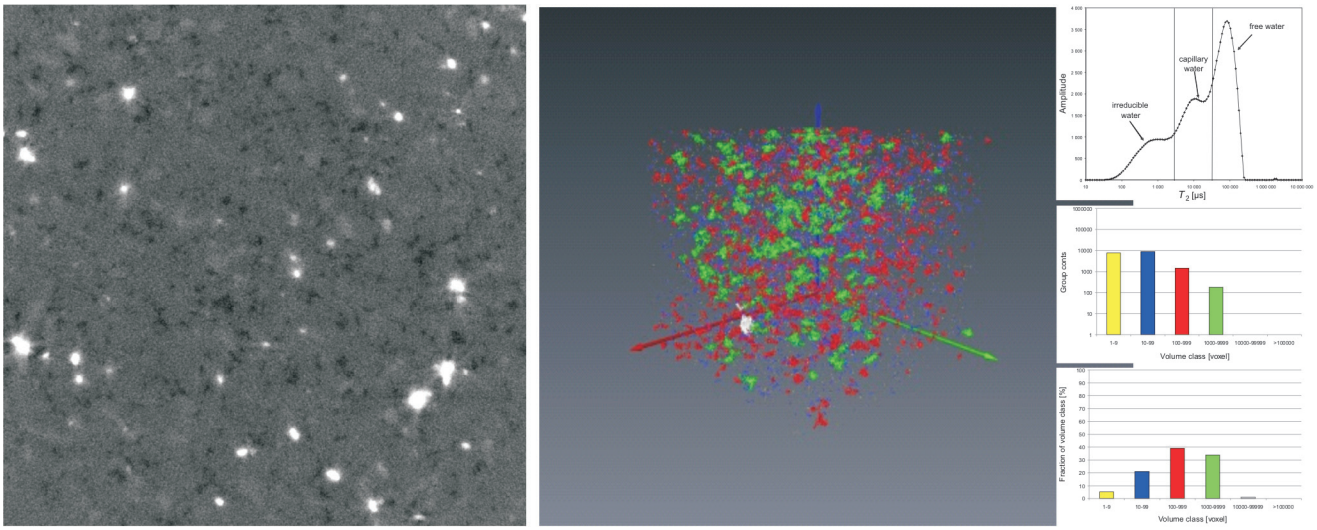

Fig. 13. Microtomographic image of sample 10744

a) cross-section through the sample; b) pore structure image

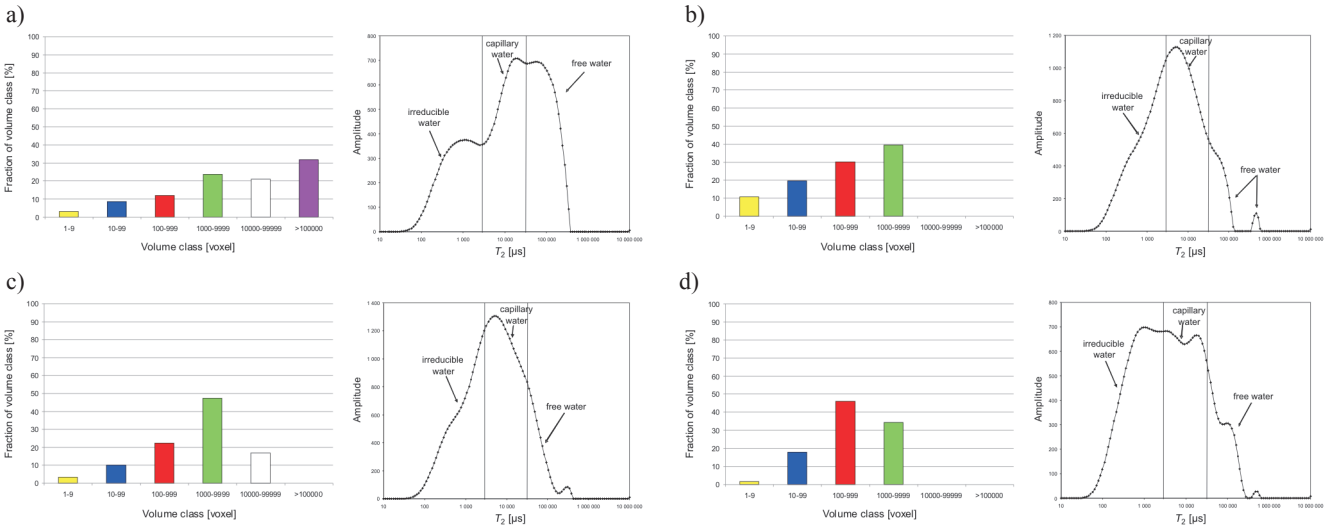

Fig. 14. Comparison of micro-CT and nuclear magnetic resonance data for selected samples from R-1 well

a) 10753 sample, A2 facies; b) 10749 sample, A2 facies; c) 10750 sample, A2 facies; d) 10752 sample, A2 facies

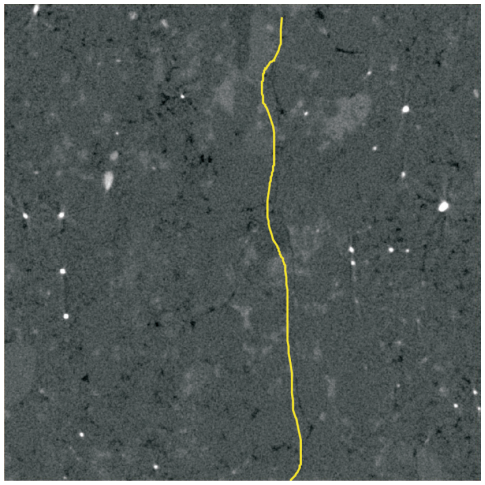

Fig. 15. Cross-section through sample 10751, illustrating narrow, intermittent fissure

Micro-CT visualization has also shown that samples originating from R-2 well feature high heterogeneity of pore distribution within pore volume (Figure 16). This heterogeneity is caused in sample 10755 by presence of the fissure, while in sample 10757 by cementation (Figure 17). The fissure mentioned above ensures relatively high permeability of sample 10755.

Samples from R-3 well represented A2 facies of dune core. Diversification of curves, reflecting the nature of their pore space has also been observed here. The first sample (10761) produces convex curve, the second sample (10758) shows concave curve, while the two remaining ones (10759, 10760) are illustrated by constant slope curve.

Tomographic images of R-3 originating samples are characterized by homogenous pore distribution and their

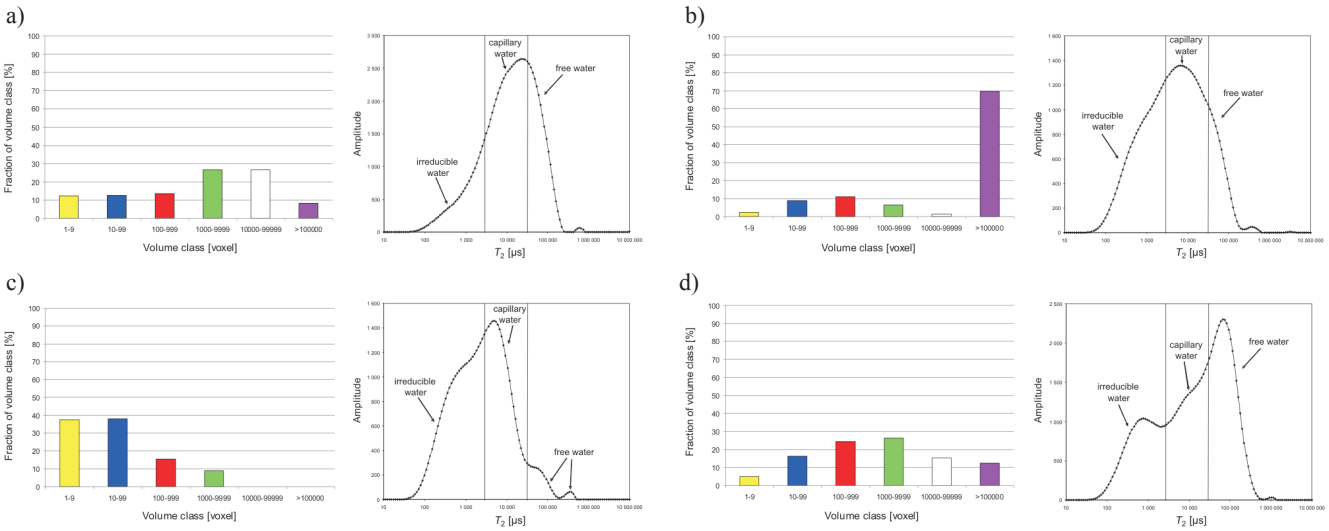

Fig. 16. Comparison of micro-CT and nuclear magnetic resonance data for samples from R-2 well

a) 10754 sample, A2 facies; b) 10755 sample, A2/A5 facies; c) 10756 sample, A2/A5 facies; d) 10757 sample, A2 facies

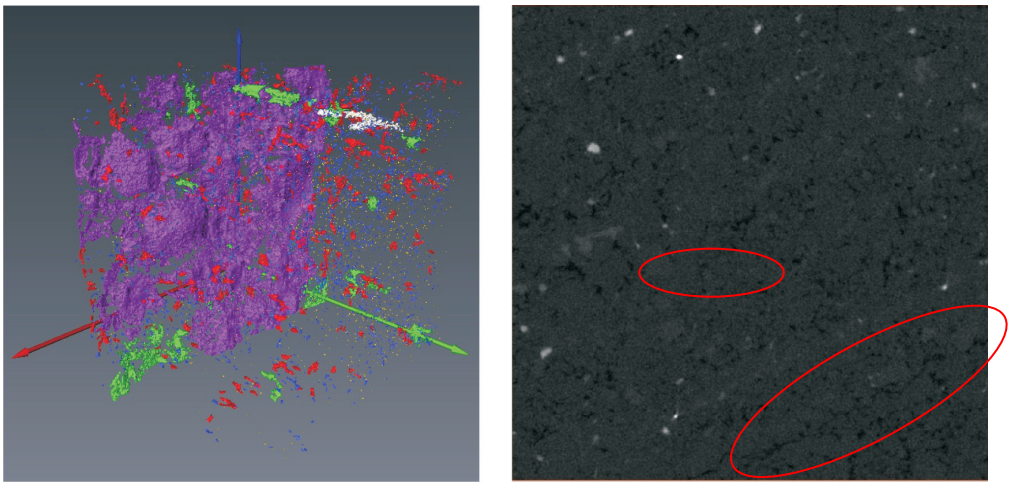

Fig. 17. Visualization of fissure in sample 10755 (on the left), and cross-section through sample 10757, with cementation areas marked on it (on the right)

reservoir properties improve with increasing depth (Figure 18). The fraction of pores belonging to volume classes I–III (volumes ranging from $2 \cdot 10^2$ to $2 \cdot 10^5$ µm^3) also decreases with depth.

Pores attributed to volume class V and VI are not present in samples 10758 and 10759 (Figure 18). Tomographic images of these samples are shown in figures 19 and 20, where the cementation increase is clearly visible.

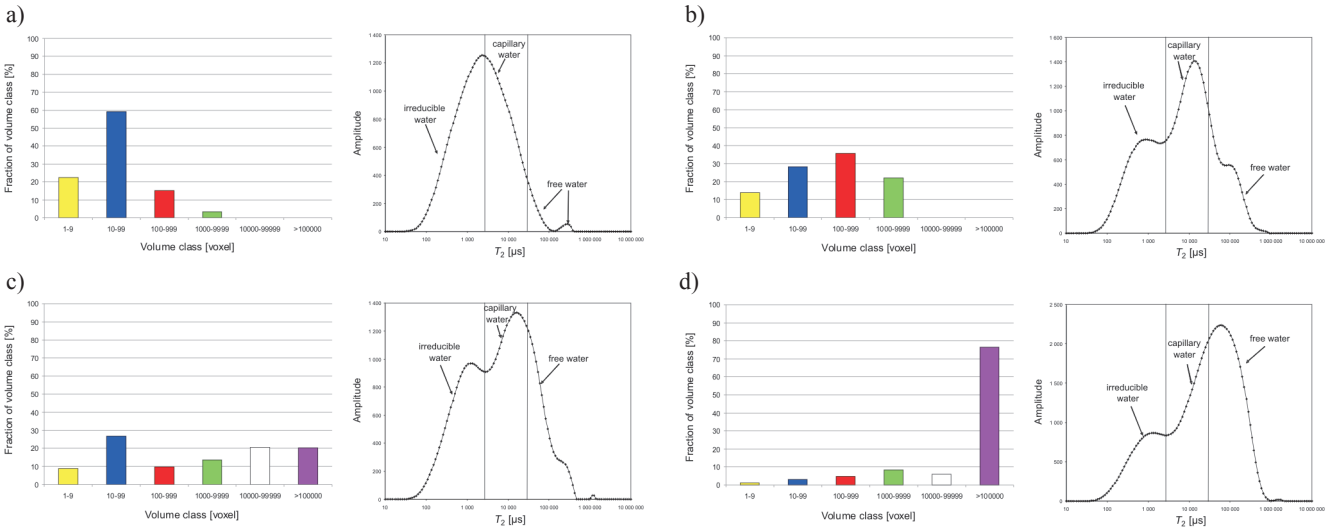

Fig. 18. Comparison of micro-CT and nuclear magnetic resonance data for samples from R-3 well

a) 10758 sample, A2 facies; b) 10759 sample, A2 facies; c) 10760 sample, A2 facies; d) 10761 sample, A2 facies

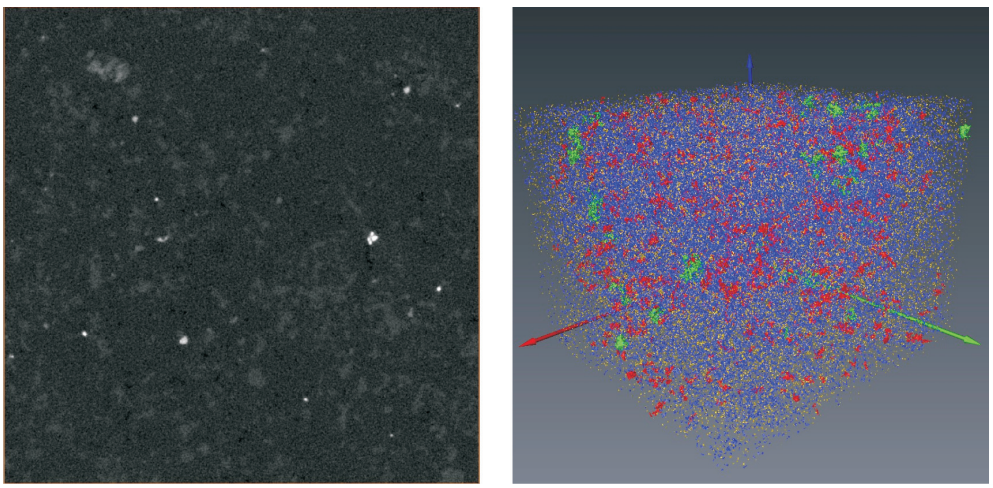

Fig. 19. Microtomographic image of sample 10758

a) cross-section through the sample (black color – pores; grey and white color – rock matrix); b) image of pore structure

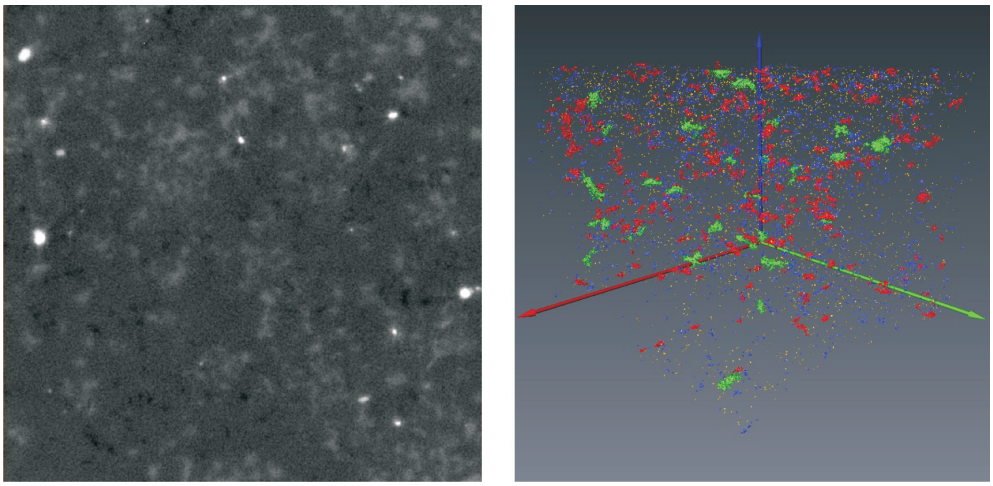

Fig. 20. Microtomographic picture of sample 10759

a) cross-section through the sample (black color – pores; grey and white color – rock matrix); b) image of pore structure

Summary

The examination results obtained with NMR method were correlated with micro-CT results. Examined samples were analyzed for:

- total and effective porosity value (using NMR method),
- irreducible, capillary and free water content (NMR method),
- value of irreducible water saturation coefficient Sw_irr,
- porosity value from micro-CT,
- distribution of porosity on micro-CT graphs,
- nature of pore network in 3D visualizations,
- permeability value,
- petrographics characteristics.

3 groups of samples, characterized by variable reservoir properties, were distinguished on the grounds of the above-listed examinations:

- group 1 – having good reservoir properties,
- group 2 – having weak reservoir properties,
- group 3 – having poor reservoir properties.

12 samples representing exclusively Aeolian dune sandstones of A2 facies were attributed to the first group, having good reservoir properties. The measurement of geometrical tortuosity of pore throats has been done for all these samples, determining the paths of possible media migrations, in many cases in three analyzed directions [5], which testifies to the presence of communication between pores.

15 samples of Aeolian dune sandstones (A2 facies) and Aeolian interdune sandstones (A4 and A5 facies) were attributed to the 2nd group, having slightly weaker reservoir properties as compared to group 1. Tortuosity parameter was determined only for three samples, but only in *Z* direction, which gives the idea of hindered communication between the pores in this group of pores.

The 3rd group counts 12 samples, having poor reservoir properties. These are first of all formations of lacustrine sediments: marginal playa (P1) and sandstone playa (P2). Three samples from A2 facies and two from A4 facies have also fallen into this group. Determination of geometrical tortuosity parameter did not succeed for any of these samples, which proves lack of communication between pores.

It can be generally stated that examined samples show significant differences in the nature of pore network and its saturation. It has been found that Aeolian dune (A2) and interdune (A4, A5) sandstones had decidedly better reservoir parameters than sediments of lacustrine facies (P1, P2) – which has been confirmed both with micro-CT and NMR examinations. This conclusion is not new and was presented earlier in the Leśniak et al. [2] study.

NMR and micro-CT examinations enabled pore space characterization of Aeolian sediments and Upper Rotliegend playa sediments. Correlation of measured parameters in vertical sections of examined wells, as well as the trial of spatial determination of reservoir properties variations in the region located in North and North-West of Poznań have also been undertaken.

Playa lacustrine sediments

The playa system is mainly composed of fine-clastic sediments (siltstones, mudstones, claystones) with secondary fraction of sandstones. Playa sediments were found in two wells of analyzed zone: G-1 and O-3. Lacustrine playa formations within the section of these wells are represented by sandy playa P2 facies (4 samples) and marginal playa P1 facies (1 sample). On the grounds of obtained results [2], playa sandstones can be depicted as fine- and very fine grain sandstones, of the lowest diameter and well sorting.

Within the whole section of G-1 well, samples of the lowest porosity, both total and effective, represent sandy playa P2 facies (10733 sample Kp_{NMR} = 3.74%, Kp_{NMR_ef} = 1.44%; 10734 sample Kp_{NMR} = 3.67%, Kp_{NMR_ef} = 0.48%). Permeability amounts to 0.539 and 0.203 respectively, for both above-listed samples. Moreover, the pores observed with micro-CT method (resolution of the method 5.8 μm in each direction) are not present in these samples. The contents of matrix type cement in sample 10734 amounts to 29.7% vol., which qualifies it as sub-arcosic wacke. The matrix constitutes here a mixture of quartz silt, allogenic clay minerals and ferrum hydroxides. The presence of authigenic clay minerals in the form of fibrous illite has also been noted [2]. According to quantitative X-ray analysis of mineral composition, quartz contents amounts to Q_{avg} = 58% and feldspars Sk_{avg} = 17%, while average contents of clay minerals is equal to 10%.

Total porosity of sample 10746 belonging to P2 facies in O-3 well amounts to Kp_{NMR} = 2.59%, effective porosity Kp_{NMR_ef} = 0.42%, and permeability Kpr = 0.321 mD. This sample has the worst parameters among all the samples being analyzed. Classes featuring the lowest pore volume predominate within the pore network of the rock sample, therefore geometrical tortuosity of pore throats was not determined. Considering the matrix type cement contents (21.7% by volume), the sample was determined as sub-arcosic wacke. The matrix constitutes here a mixture of quartz silt, allogenic clay minerals and ferrum hydroxides [2]. According to quantitative X-ray analysis of mineral composition, quartz contents amounts to Q_{avg} = 62% and feldspars Sk_{avg} = 18%, while the sum of clay minerals is equal to 13%. Marginal playa P1 facies is represented by sample 10745. By definition, P1 facies formations are finegrain sandstones (of transit zone) which differ significantly from P2 facies formations resembling dune core facies (A2) in their development. Total porosity of sample 10745 amounts to Kp_{NMR} = 6.54%, effective porosity Kp_{NMR_ef} = 3.25%, and porosity reaches 1.015 mD. However, classes of the lowest pore volume predominate in the pore network of the rock sample. The pores for which calculation of tortuosity would be possible are not present. The sample was depicted as sub-arcosic arenite [2]. According to quantitative X-ray analysis of mineral composition, quartz contents amounts to Q_{avg} = 73% and feldspars Sk_{avg} = 20%, while the sum of clay minerals is equal to 5%.

Aeolian sediments

R region was represented by three boreholes R1, R-2, and R-3. Aeolian sandstones are present in sections of these boreholes: dune facies – of dune core (A2) and interdune facies – of sandy cover (A4) and dry interdune zone (A5). In terms of grain size analysis, the rocks can be specified as fine- and very fine-grained sandstones. Originally, these were very good and good reservoir rocks. Aeolian sediments are currently characterized by moderate and weak filtration properties. Average value of total porosity for this region, determined on the grounds of 13 rock samples examination is equal to Kp_{NMR} = 9.98%, effective porosity Kp_{NMR_ef} = 6.38%, and average permeability reaches 11.38 mD. Although their reservoir properties are not so bad, the Aeolian sandstones from R region have the poorest parameters according to these examination results.

NMR method examination results indicated the lowest average value of effective porosity and the highest average value of irreducible water saturation coefficient ([4] – Table 6, Figure 4). Also, the results obtained from micro-CT data analysis have been found as the poorest in this region, which is presented in the summary of percentage fraction of individual pore size classes ([5] – Table 3). There is a small number of volume class VI pores in A2 facies formations of rock samples' pore network, classes I–III predominate (pore assembly of $2 \cdot 10^2 \div 2 \cdot 10^5$ μm^3 volume), class IV–V pores are scarce. The analysis of pore throats tortuosity results for samples from this region gave the highest values, which testifies to a more complex shape of pore structure ([5] – Table 4). Negative results of fluids flow simulation trials through selected rock samples only confirmed heterogeneous nature of the pore structure.

It can be observed when preparing the graphs of total and effective porosity coefficient value changes with depth for R-1, R-2, and R-2 wells, that the development of pore space parameters correlates with porosity [2]. In every place where porosity reaches high values, medium pores (volume class IV, V) predominate in the pore network of rock samples, and the samples are characterized by uniform distribution of pores. Examinations in the scope of pore throats geometrical tortuosity reveal connections between opposite walls, however not in all directions. The trend of reservoir properties improvement with depth can be observed. An exception are the samples in which distinct increase of clay minerals contents in rock sample pore space is noted (R-1, sample 10752; R-2, sample 10756; R-3, sample 10759). What should also be noted is the occurrence of decreased porosity spherical areas in majority of the samples, which gives evidence of the presence of cement.

As results from the qualitative evaluation of rock mineral composition with the X-ray phase analysis method,

the main constituents of examined rock samples are quartz Q_{avg} = 72% (the highest average quartz contents among all analyzed rock samples) and feldspars Sk_{avg} = 10% (the lowest feldspar contents among all the analyzed rock samples). The clay content level strongly varies. The highest content of clay minerals has been found in samples from R region (Σ_{clay_avg} = 12,5%). The highest clay content – 16%, has been observed in A2 facies samples from R region (R-1, sample 10752, R-3, sample 10759).

The samples of A2 facies in G-1 borehole feature average total porosity value Kp_{NMR} = 11.81% and effective porosity value Kp_{NMR_ef} = 8.67%. The samples of A2 facies from this borehole feature slightly lower average effective porosity value as compared to O-3 borehole, while average value of irreducible water saturation coefficient is higher ([4] – Table 6). This is confirmed with micro-CT examination results, contained, among others, in tabular summary of individual pore classes percentage fraction ([5] – Table 1) as well as geometric tortuosity of pore throats ([5] – Table 4). Average permeability amounts to 5.81 mD (min. 1.249, max. 15.137) [2]. These formations feature relatively good parameters. According to the results of micro-CT examination these are samples of well developed internal pore network (10730, 10729, 10727, 10726) and are characteristic in that class VI of pore volume predominates. Distribution of pores is heterogeneous, which is evidenced by large porosity difference between subsamples (for example in sample 10726). Determination of pore throats tortuosity was successful for three samples (10726, 10729, 10730), but not in all directions. Only for samples 10729 and 10726 these connections have similar pore throats tortuosity in all main directions *X*, *Y*, *Z*, while good transport properties of these samples are owing to pores of class VI as well.

Similarly as in case of G-1 well, in O-3 well under sandy playa of P2 facies, Aeolian sandstones mainly of A2 facies are present, and secondarily interdune facies sandstones (A4). Samples from this well are distinguishable by the best reservoir properties within the whole analyzed area, and average value of irreducible water saturation coefficient is the lowest. The same information is contained, among others, in tabular summary of individual classes percentage fraction ([5] – Table 2) as well as geometric tortuosity of pore throats determined with micro-CT method ([5] – Table 4). For 12 examined samples, as many as 5 have been counted among the group of good reservoir properties. This is also confirmed by comparison of changes and average values of parameter ranges determined with NMR method and permeability for A2 facies formations ([4] – Table 6). Average value of total porosity Kp_{NMR} = 12.19% and effective porosity amounts to Kp_{NMR_ef} = 9.38%. Average permeability amounts to 29.98 mD (min. 3.464 mD, max. 110.013 mD) [2]. The same information is contained in percentage fraction of individual classes. As many as 6 samples are characterized by well developed internal pore network, where pore volume class VI predominates. Four samples had moderately developed pore structure (samples originating from various facies A2, A4, A5). In pore network of the rock samples small and medium pores predominate here (volume class II and III), and the samples are characterized by non-uniform pore distribution. Examinations in the scope of pore throats geometric tortuosity were done for five samples. Connections between opposite walls have been found in two samples, 10743 and 10737. Good transport properties were provided by class VI pores, while tortuosity parameter determined for these samples amounts to 1.3, which gives evidence to near straight connection of the opposite walls. The connections in the remaining samples do exist, however not in all directions.

Complex diagenetic processes (mechanical compaction and cementation, as well as substitution and grain transformation processes) occurring in this area led to significant deterioration of reservoir properties. Mechanical compaction was the longest acting diagenetic process. It negatively influenced the original porosity of sandstones. The packing of matrix grain has been increasing, and intergranular space reducing in the result of compaction action [2]. Cementation with carbonate minerals, sulfate minerals, as well as cementation with authigenic quartz has led to a dramatic decrease of Aeolian sandstones original porosity.

Conclusions

The best petrophysical parameters in aspect of media accumulation and migration were obtained for A2 facies Aeolian dune sandstones, and slightly weaker for A4 facies interdune sandstones assembly. It results from micro-CT data that A2 facies formations were characteristic in that class VI of pore volumes was present in all samples (assembly of pores of volume in excess of $2 \cdot 10^7$ µm^3) – the volume class that frequently predominated or was present together with the second predominant of class V. These sandstones featured a large number of high class pores and low fraction of pore volume classes I–III (pore assembly of $2 \cdot 10^2 \div 2 \cdot 10^5$ µm^3 volume). It can be stated

on the grounds of NMR data that these samples were characterized by the highest values of total and effective porosity and high percentage of free water content, as well as the lowest coefficient of irreducible water saturation.

The worst reservoir properties were characteristic for P2 sandy playa facies and P1 marginal playa, exhibiting total lack of the highest, class VI (pore assembly of volume in excess of $2 \cdot 10^7$ µm^3) of pore volume. The pores create subgroups of sizes ranging from classes I to III (pore assembly of volume $2 \cdot 10^2 \div 2 \cdot 10^5$ µm^3), with modal value present mainly in class II and sometimes in classes III or I. Micro-CT observations are confirmed by NMR results, according to which these samples were characterized by the lowest total and effective porosity values and free water content, while the coefficient of irreducible water saturation was the highest.

The article was sent to the Editorial Section on 18.02.2011. Accepted for printing on 4.08.2011.

Reviewer: prof. zw. dr hab. inż. Andrzej Kostecki

References

[1] Jarzyna J., Puskarczyk E., Wójcik A., Semyrka R.: *NMR as well as porosimetric measurements on selected rock samples from West Carpathians*. Geology, vol. 33, book 4/1, p. 211–236, 2007.

[2] Leśniak G. et al.: *Determination of processes leading to creation of anomalously low porosity and permeability in Aeolian sandstones in the Poznań-Kalisz-Konin region, as well as perspectives of discovering "tight-gas" type reservoirs in this zone*. Documentation of 395/SG work, archive Oil and Gas Institute, 2009.

[3] Zalewska et al.: *Pore space evaluation of Upper Rotliegend sandstones in G-R region with the use of nuclear magnetic resonance and X-ray computed microtomography methods*. Documentation of 454/SW work, archive of Oil and Gas Institute, 2010.

[4] Zalewska J., Cebulski D.: *The analysis of rock pore space saturation distribution with nuclear magnetic resonance method (part II)*. Nafta-Gaz No. 9, 2011.

[5] Zalewska J., Kaczmarczyk J.: *The analysis of rock samples internal pore structure based on X-ray computed microtomography data (part I)*. Nafta-Gaz No. 8, 2011.

MSc Eng. Jadwiga ZALEWSKA – geologist, Academy of Mining and Metallurgy alumna. Head of Well Log Geophysics Department in Oil and Gas Institute – Krakow. Accomplishes research and development works in scope of laboratory measurements of drilling cores and muds for quantitative interpretation of well logs. Author of 132 published works.

MSc. Marek DOHNALIK – Master of Environmental Engineering at Krakow University of Technology. Employed in Well Logging Department of Oil and Gas Institute. Since 2008 specializes in the study of rocks with the use X-ray microtomography.